Neuroanatomical correlates of intellectual ability across the life span

Suzanne Goh*, Ravi Bansal, Dongrong Xu, Xuejun Hao, Jun Liu, Bradley S. Peterson

Columbia University Medical Center and New York State Psychiatric Institute, 1051 Riverside Drive, Unit 74, New York, NY 10032, United States

ARTICLE INFO

ABSTRACT

Attempts to correlate measures of intellectual ability with localized anatomical imaging features of the brain have yielded variable findings distributed across frontal, parietal, and temporal lobes. To better define the gray and white matter correlates of intellectual ability and the effects of sex and age, we analyzed the brains of 105 healthy individuals, ages 7–57 years, who had a Full Scale Intelligence Quotient (FSIQ) of 70 or higher. We examined associations of FSIQ with cortical thickness and with white matter volume throughout the cerebrum. Thinning of left ventromedial and right dorsolateral prefrontal cortices correlated significantly with FSIQ. Sex modified correlations of cortical thickness with FSIQ in the left inferior frontal, left cingulate, and right dorsomedial prefrontal cortices. Correlations of local white matter volumes with FSIQ varied by age, with adults showing inverse correlations of white matter volume with FSIQ in a large territory of right frontal white matter likely corresponding to fiber tracts of the superior corona radiata and superior longitudinal fasciculus. These findings corroborate the role of frontal and parietal association cortices and long association white matter fibers in higher intelligence and suggest ways in which the neuroanatomical correlates of higher intelligence may vary by sex and age.

© 2011 Elsevier Ltd. All rights reserved.

1. Introduction

Intellectual ability has been defined in broad terms as the "ability to understand complex ideas, to adapt effectively to the environment, to learn from experience, to engage in various forms of reasoning, [and] to overcome obstacles by taking thought" (Neisser et al., 1996). Whether such an expansive human capacity can be quantified by a single numerical index and ascribed a localized neurobiological substrate has been a topic of interest and debate for at least two centuries (Deary et al., 2010; Gould, 1981).

Brain imaging studies have identified normal variability in anatomical and functional characteristics of the brain, particularly in parietal and frontal regions, that seem to underlie inter-individual differences in intellectual ability. Most anatomical imaging studies have correlated psychometric measures of intelligence, primarily the full-scale intelligence quotient (FSIQ), with measures of gray or white matter volumes (Luders et al., 2009). Features of the dorsolateral prefrontal cortex, anterior cingulate gyrus, and inferior parietal cortex have shown the most consistent correlations, with approximately 30–40% of studies reporting significant findings in these areas (Jung and Haier, 2007). These findings have motivated formulation of a "Parieto-Frontal Integration Theory of Intelligence," which posits that multimodal association cortices and their connections, within primarily the frontal and parietal lobes, underlie intellectual ability (Jung and Haier, 2007).

Techniques for measuring cortical thickness have recently been applied to the study of intellectual ability. These may provide more refined, localized, and valid measures of the cytoarchitectural features of the brain that support learning and memory processes and, therefore, also intelligence (Peterson, 2010). Four prior studies

* Corresponding author at: 1051 Riverside Drive, Unit 74, New York, NY 10032, United States. Tel.: +1 415 317 4514; fax: +1 201 224 3925.
E-mail addresses: gohs@childpsych.columbia.edu, suzgoh@gmail.com (S. Goh), bansalr@childpsych.columbia.edu (R. Bansal), xud@childpsych.columbia.edu (D. Xu), haox@childpsych.columbia.edu (X. Hao), liuj@childpsych.columbia.edu (J. Liu), petersob@childpsych.columbia.edu (B.S. Peterson).

have examined correlations of cortical thickness with measures of intelligence. A cross-sectional study of 65 young adults demonstrated positive correlations of FSIQ with cortical thickness in the prefrontal and posterior temporal cortices, with sex influencing regional correlations (Narr et al., 2007). A longitudinal study of 307 children reported that participants who had higher FSIQ scores showed an accelerated and prolonged phase of cortical thickening within the prefrontal cortices, followed by vigorous cortical thinning in early adolescence (Shaw et al., 2006). A cross-sectional study of 216 children and adolescents reported correlations of intelligence with measures of cortical thickness distributed in multimodal association cortices throughout the brain (Karama et al., 2009). A cross-sectional study of 225 young adults demonstrated correlations of cortical thickness with measures of crystallized intelligence in the left temporal lobe, and correlations of fluid intelligence with neural activity in prefrontal cortices (Choi et al., 2008). No study has yet examined correlations of FSIQ with cortical thickness across the life span or included concurrent analyses of local white matter volumes.

We measured cortical thickness throughout the cerebrum in 105 healthy children and adults, ages 7–57. We assessed correlations of cortical thickness with FSIQ and examined the moderating effects of sex and age. We then examined regional white matter volume to determine whether cortical findings were accompanied by differences in white matter volume.

2. Methods

2.1. Participants

We recruited healthy adults and children selected randomly from a telemarketing database. All participants were recruited as controls for imaging studies of adult and childhood neuropsychiatric disorders. Introductory letters were sent and then followed by screening telephone calls. A detailed clinical interview was performed that included the Kiddie-Schedule for Affective Disorders and Schizophrenia (Kaufman et al., 1997) for children and the Structured Clinical Interview for DSM-IV Axis I Disorders (Spitzer et al., 1992) for adults. Individuals with a current or past history of a psychiatric or neurological disorder were excluded.

Our sample included 105 participants with FSIQ of 70 or higher who ranged in age from 7 to 57 years (mean 17.7 years, SD: 11.2 years). The sample was similarly distributed across gender (females 45.7%) and was predominantly right-handed (96.2%). Children under 18 years of age comprised 62% of the sample (Table 1).

2.2. Neuropsychological assessment

Because healthy participants were recruited as controls for several different studies, intelligence testing was performed using different instruments depending on the research study protocol. For the vast majority of participants ($n = 85$), intelligence testing was performed using the age-appropriate version of the Wechsler intelligence scales: Wechsler Intelligence Scale for Children, 3rd edi-

Table 1
Demographic and FSIQ data for the participants.

		Range	Mean	SD
Females	Age (y)	7–57	18.9	13.2
($n = 48$)	FSIQ	89–154	118.3	16.1
Males	Age (y)	7–57	18.2	11.8
($n = 57$)	FSIQ	70–150	119.4	16.4
Children	Age (y)	7–17	10.6	2.4
($n = 65$)	FSIQ	70–154	115.5	16.7
Adults	Age (y)	18–57	30.8	11.0
($n = 40$)	FSIQ	96–150	125.9	14.7
All	Age (y)	7–57	17.7	11.2
participants ($n = 105$)	FSIQ	70–154	120.5	17.2

tion (WISC-III) ($n = 51$) or Wechsler Adult Intelligence Scale Revised (WAIS-R) ($n = 34$). For children tested with the WISC-III, FSIQ was estimated using established abbreviated forms that correlate .90 or above with scores from the full administration (Kaufman et al., 1996). Three children and six adults were evaluated with the Wechsler Abbreviated Scale of Intelligence (WASI) using the four-subtest format. FSIQ correlations between the WASI and longer forms have been established at .87–.92 (Psychological Corporation, 1999). Eleven children were evaluated with the Kaufmann Brief Test of Intelligence (K-BIT). Correlations of the K-BIT with WISC-III have been established at .89 (Canivez et al., 2005). Although different instruments were used to calculate FSIQ (in part, because of the wide age range of participants and, in part, because of differing study protocols), all instruments have been shown to correlate highly with one another and to test similar domains of cognitive function. To ensure that IQ test type did not influence the findings, we performed all analyses both with and without the nine individuals assessed with the WASI and the 11 children assessed with the KBIT. We compared correlation coefficients and p-values from the separate analyses. Because we detected no differences in the statistical significance of the findings, all individuals were included in the final analysis. In addition, we assessed the scatterplots for regressions with each of the IQ instruments to ensure that none of the instruments altered the overall trajectory of the regression lines.

Intelligence testing was generally performed on the same day as the MRI scan and always occurred within 1 month of the MRI scan. Three individuals with no identifiable neurological disorder had FSIQ between 70 and 80. To ensure that these individuals did not exert excessive influence on the findings, all analyses were performed with and without these individuals. Again, we compared correlation coefficients and p-values from the separate analyses, and because we detected no differences in the statistical significance of the findings, these three individuals were included in the final analysis.

2.3. Image acquisition and processing

2.3.1. MR image acquisition

Anatomical images were acquired for each participant using a 1.5 Tesla Scanner (GE Signa; General Electric, Milwaukee, WI). Head positioning was standardized using cantho-meatal landmarks. Images were acquired using a three-dimensional spoiled gradient recall sequence with

the following parameters: repetition time (TR) = 24 ms, echo time (TE) = 5 ms, 45° flip angle, matrix size 256 × 192, 2 excitations, field of view (FOV) 30 cm, 124 contiguous sagittal slices 1.2 mm thick without skip and reformatted with voxel dimensions 1.17 mm × 1.17 mm × 1.2 mm.

2.3.2. MR image processing

Brains were isolated from non-brain tissue using an automated tool for brain extraction followed by manual editing (Shattuck and Leahy, 2002). Cortical gray matter was defined using a combination of thresholding of representative values of gray and white matter together with hand editing in all three orthogonal views on Sun Ultra 10 workstations using ANALYZE 7.5 software (Rochester, MN). The gray scale values of "pure" representations of cortical gray matter (the cortical ribbon) and white matter were sampled bilaterally at 4 standard locations throughout the brain (frontal, temporal, occipital, and parietal regions) using an $8 \times 8 = 64$ pixel array – one that is sufficiently large to provide statistical stability but small enough to avoid partial volume effects that include other tissue types. These 4 values were then averaged for each tissue type. A global threshold whose value was halfway between the mean gray matter and mean white matter values was then invoked to provide an initial rough classification of cortical gray and white matter throughout the cerebrum. This classification was then hand edited in all 3 views, primarily to eliminate subcortical gray matter and the rims of the ventricles (partial-volumed white matter and ventricular CSF that is labeled as gray matter in most segmentation algorithms) from the tissue assigned to cortical gray matter. White matter was defined by the subtraction of all other structures (cortical gray, subcortical gray, and ventricular CSF) from the isolated cerebrum. Analysts were blind to participant characteristics and hemisphere (images were flipped randomly left-right prior to region definition to eliminate the effects of perceptual bias on lateralized measures). Flips were corrected prior to distance measurements. Inhomogeneities in image intensity were removed prior to isolation of cerebral tissue (Sled et al., 1998). Interrater reliabilities, calculated as intraclass correlation coefficients using a two-way random effects model, were all >.98 (Arndt et al., 1991).

2.3.3. Template selection

Detailed descriptions of the procedures used to analyze surface morphologies and of related validation studies are provided elsewhere (Bansal et al., 2005). To select the most appropriate, representative template brain for surface morphometry, we first selected as a preliminary template brain the participant who demographically most representative of all healthy controls. The brains for all remaining participants were coregistered to this preliminary template using a rigid body similarity transformation (3 translations, 3 rotations, and a global scale). The coregistered brains were then nonlinearly transformed to the template brain by a high-dimensional, non-rigid warping algorithm based on fluid dynamics (Bansal et al., 2005; Wells et al., 1996). Each brain, thus, was warped to the exact same size and shape as the template brain, permitting identification of points on the surface of each brain that

corresponded precisely with those of the template brain. After the point correspondences on the cerebral surfaces were determined, we computed distances between the corresponding points. Then the cerebrum for which all points across its surface were closest, in terms of least squares, to the average of the computed distances was selected as the final template. The coregistration (rigid body similarity transformation), application of the non-rigid warping algorithm based on fluid dynamics, and determination of point correspondences were then repeated for all participants prior to statistical modeling. The use of a single representative brain as a template rather than an averaged brain from many individuals enables greater accuracy of registration. A single brain has sharp borders at tissue interfaces, such as the CSF-gray matter interface at the cerebral surface, or the gray-white interface at the cortical mantel. In our experience, averaging images for a template blurs these boundaries and increases registration errors that are subtle but important when distinguishing subtle effects across populations. In addition, precise surface morphometry requires a brain with smooth gray and white surfaces that are devoid of topological defects, which cannot be reconstructed by averaging brains from many individuals.

2.3.4. Calculating cortical thickness

From the coregistered brain of each participant, we subtracted its cortical mantel. We then used a three-dimensional morphological operator to distance-transform this brain without the cortex from the coregistered brain of the same participant that contained cortex. This operation calculated cortical thickness as the smallest distance of each point on the external cortical surface from the outermost surface of the white matter in the coregistered brain. These measurements of cortical thickness were not performed in the native space of untransformed brains, but rather on brains that had been coregistered using a rigid body similarity transformation (3 translations, 3 rotations, and a global scale); therefore, measures of cortical thickness inherently controlled for whole brain volume.

Because intelligence has been shown to correlate with total brain volume (TBV), using measures of cortical thickness in template space may remove the variance of interest in our analyses. We therefore also performed all statistical analyses using measures of cortical thickness in native space. These results were similar to the results of analyses performed using measures in template space; therefore, we present below only the results from analyses in template space.

We used multivariate linear regression at each point on the reference surface to examine associations of FSIQ with cortical thickness. In addition to main effects, we considered for inclusion in the model all 2-way interactions of age, sex, and FSIQ: $t_i = \beta_0 + \beta_1 \times age + \beta_2 \times age^2 + \beta_3 \times sex + \beta_4 \times age \times sex + \beta_5 \times FSIQ + \beta_6 \times FSIQ \times sex + \beta_7 \times FSIQ \times age + \beta_8 \times FSIQ \times age^2$ (where t_i is the set of cortical thickness measurements for all participants). The model was hierarchically well formulated (all lower-order component terms were included in the model, regardless of statistical significance). We used the theory of Gaussian Random Fields (GRFs) to account for the multiple correla-

tions computed across the cortical surface (Bansal et al., 2007). We computed the correlation between cortical thickness (t_i) and FSIQ, and we evaluated the p-value of this correlation using a Student's t-test. Statistical maps were generated by displaying color-coded p-values across the entire surface of the cortex. Statistical maps were also generated for the FSIQ-by-sex and FSIQ-by-age interactions. Following correction for multiple comparisons, no cortical regions showed statistically significant FSIQ-by-age or FSIQ-by-age^2 interaction. These terms were, therefore, removed from the regression model in the final analysis. We generated scatterplots for areas of significant FSIQ-by-sex interaction to characterize further the influence of sex.

2.4. Volume-preserved warping

Using the deformation field that normalizes brains into the template space in surface analyses, VPW warps a binarized image of the brain to generate a spatially normalized image with varying pixel intensities. In this normalized image, regions of high intensity denote regions compressed by the deformation field, and the regions of low intensity denote regions that were expanded by the deformation field. Thus, regions of high VPW intensity are those that have greater volume in the participant's brain than in the template brain, and regions of low VPW intensity are those that reduced volume in the participant's brain relative to the template brain. We then perform voxel-wise statistical analyses to detect regions of significant correlation between local brain volumes and FSIQ. These methods have been described extensively elsewhere (Davatzikos et al., 2001; Xu et al., 2007).

3. Results

3.1. Cortical thickness

We detected significant inverse correlations of cortical thickness with FSIQ in bilateral prefrontal regions after correction for multiple comparisons: left anterior cingulate gyrus (BA 32), left orbitofrontal cortex (BA 10, 11), left subgenual gyrus (BA 25), and right middle frontal gyrus (BA 46) (Fig. 1). No other regions of significant FSIQ main effect were detected.

Several cortical regions, primarily in the frontal lobes, showed a significant FSIQ-by-sex interaction following correction for multiple comparisons (Fig. 2). In the left hemisphere, these regions included the inferior frontal cortex (IFC) (BA 44, 45), anterior cingulate cortex (ACC) (BA 24), and posterior cingulate cortex (PCC) (BA 29, 30, 31). In the right hemisphere, a significant interaction was detected in the right superior frontal gyrus (BA 8, 9). In general, the sign of the correlation coefficient between FSIQ and cortical thickness was positive for females and negative for males. An exception was the left anterior cingulate cortex, where cortical thickness correlated positively with FSIQ in males and inversely in females.
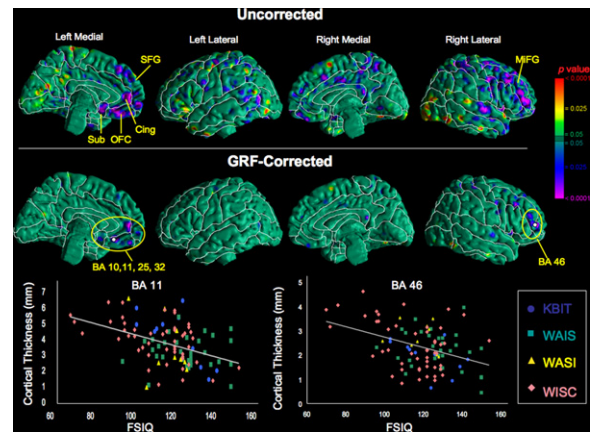

Fig. 1. Correlations of cortical gray matter thickness with FSIQ in all participants ($t_i = \beta_0 + \beta_1 \times age + \beta_2 \times age^2 + \beta_3 \times sex + \beta_4 \times age \times sex + \beta_5 \times FSIQ + \beta_6 \times FSIQ \times sex$, where t_i is the set of cortical thickness measurements for all participants). The color bar indicates the statistical significance of the correlations (purple, negative correlation; red, positive correlation). On the uncorrected maps, gyri with prominent regions of high statistical significance ($p < .0001$) are labeled: left superior frontal gyrus (SFG), left cingulate gyrus (Cing), left orbitofrontal cortex (OFC), left subgenual region (Sub), and right middle frontal gyrus (MiFG). On the GRF-corrected maps significant Brodmann areas are labeled ($p < .0001$): BA 10, 11, 25, and 32 on the left ($r^2 = .16$) and BA 46 on the right ($r^2 = .20$). The brain was scaled during the similarity transformation to the template brain; therefore, measures of cortical thickness inherently accounted for generalized scaling effects within the cerebrum. (For interpretation of the references to color in this figure legend, the reader is referred to the web version of the article.)
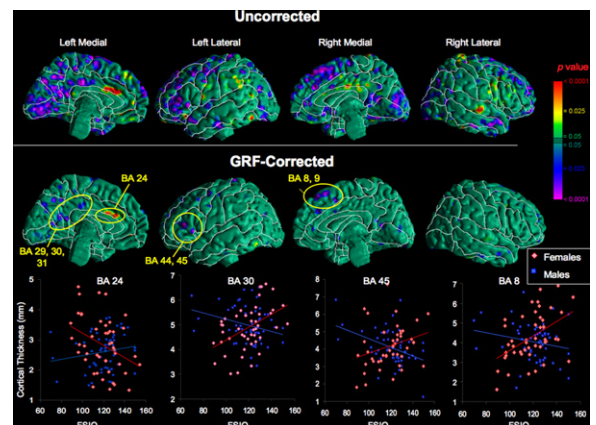

Fig. 2. Cortical regions of significant FSIQ-by-sex interaction ($t_i = \beta_0 + \beta_1 \times age + \beta_2 \times age^2 + \beta_3 \times sex + \beta_4 \times age \times sex + \beta_5 \times FSIQ + \beta_6 \times FSIQ \times sex$, where t_i is the set of cortical thickness measurements for all participants). The color bar indicates areas of significant FSIQ-by-sex interaction. On the GRF-corrected maps Brodmann areas with significant FSIQ-by-sex interaction are labeled ($p < .0001$): BA 24, 29, 30, 31, 44, and 45 on the left and BA 8 and 9 on the right. In nearly all regions of significant FSIQ-by-sex interaction, females show a significant positive correlation of FSIQ with cortical thickness, whereas males show an inverse correlation. An exception is the left anterior cingulate cortex (BA 24) where the correlation is positive in males and negative in females. For females, all correlations are significant ($p < .05$); for males, correlations are significant in the left posterior cingulate cortex and left inferior frontal cortex. Partial effects of age have been removed. (For interpretation of the references to color in this figure legend, the reader is referred to the web version of the article.)
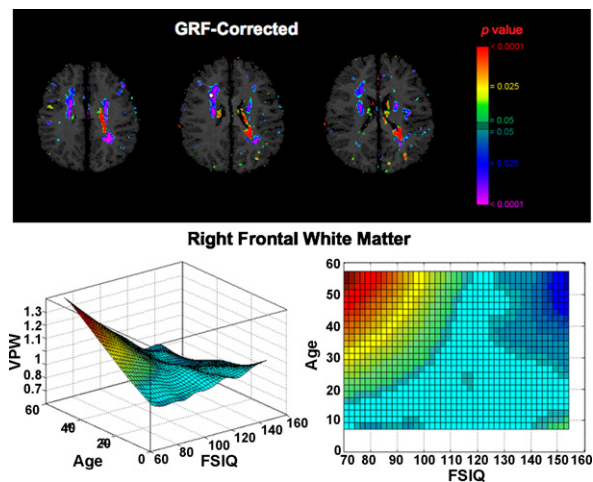
Fig. 3. Regions of significant FSIQ-by-age interaction in analyses of tissue contraction or expansion using volume-preserved warping ($VPW_i = \beta_0 + \beta_1 \times age + \beta_2 \times age^2 + \beta_3 \times age^3 + \beta_4 \times sex + \beta_5 \times age \times sex + \beta_6 \times FSIQ + \beta_7 \times FSIQ \times sex + \beta_8 \times FSIQ \times age$, where VPW_i is the set of tissue volume measurements). VPW warps a binarized image of the brain to generate a normalized image with varying pixel intensities. In this normalized image, regions of high intensity denote the regions compressed by the deformation field, and regions of low intensity denote the regions that were expanded by the deformation field. The color bar indicates the statistical significance of the interaction. A large territory of right frontal white matter shows significant FSIQ-by-age interaction. This interaction is shown in the three-dimensional graph, where greater VPW intensity is denoted in red color and reflects greater tissue volume, and blue-green colors indicate reduced VPW intensity and smaller tissue volumes. In the right frontal lobe, adults show inverse correlations of FSIQ with white matter volume, whereas in children no correlation is detected. (For interpretation of the references to color in this figure legend, the reader is referred to the web version of the article.)

3.2. White matter

To examine correlations of FSIQ with local volumes of white matter tissue, we performed exploratory analyses of tissue contraction or expansion associated with FSIQ using volume-preserved warping (VPW). We detected a prominent region of significant FSIQ-by-age interaction on VPW measures in right frontal white matter, including the region of white matter underlying the area of cortical thinning in the right DLPFC (Fig. 3). Post hoc analyses showed that FSIQ correlated inversely with white matter volume in this region in adults but not in children. We also detected a significant FSIQ-by-age interaction in smaller region in the left periventricular white matter, where FSIQ correlated positively with white matter volume in adults but not in children. We did not detect areas of significant FSIQ main effect or FSIQ-by-sex interaction on VPW values in white matter regions after correction for multiple comparisons. By referencing atlases of white matter anatomy generated from pathological and neuroimaging studies, we speculate that fibers from the region of significant FSIQ-by-age interaction in the right frontal white matter are likely to correspond to fibers of the superior corona radiata, superior longitudinal fasciculus, and anterior portion of the corpus callosum (Mori et al., 2005; Schmahmann and Pandya, 2006).

3.3. Total brain volume

To examine the correlation of total brain volume with FSIQ, we used a scaling factor that indicates the percentage increase or decrease in volume during the process of warping the individual brain to the template brain (i.e., a scaling factor of 1.05 indicates that the individual brain volume was scaled up by a factor of 1.05 during the process of registering the individual brain to the template). We detected a significant inverse correlation of FSIQ with this scaling factor while covarying for age and sex ($p = .05$, df = 95, $\beta = -.00033$), indicating that FSIQ correlates significantly and positively with total brain volume.

4. Discussion

In this cross-sectional study of a large sample of healthy children and adults, thinning of the left ventromedial and right dorsolateral prefrontal cortices correlated significantly with FSIQ. Moreover, sex modified correlations of cortical thickness with FSIQ in several regions, most prominently in Broca's area, the left cingulate cortex, and the right medial prefrontal gyrus. In the region of white matter underlying the right frontal cortices, age modified the correlation of FSIQ with white matter volume, with an inverse correlation present in adults and no significant correlation detected in children. Overall, our findings support the Parieto-Frontal Integration Theory of intelligence (Jung and Haier, 2007) and contribute to this model in important ways: first, by demonstrating inverse correlations of cortical thickness and FSIQ in localized regions of the prefrontal cortices; second, by demonstrating sex-specific patterns in the neural correlates of intelligence; and, third, by demonstrating both white matter and cortical thickness correlates of intelligence, thereby deepening our understanding of the possible cellular mechanisms underlying the neural correlates of intellectual ability.

The participation of prefrontal cortex (PFC) in higher cognitive functioning has been well established through neuroimaging, electrophysiological, and lesion studies in humans and animals. The PFC, which comprises Brodmann areas 8–13, 24, 32, 46, and 47, supports working memory, attentional processes, and the representation and control of actions and behavior (Wood and Grafman, 2003). The PFC matures later than other cortices, with myelination and synaptic pruning accelerating through adolescence (Benes et al., 1994; Gogtay et al., 2004; Huttenlocher, 1990; Huttenlocher and Dabholkar, 1997; Sowell et al., 1999a, 1999b). Structural maturation of the PFC involves both cortical thinning as well as increases in regional volume, probably from localized increases in white matter volume (Giedd et al., 1999; Jernigan et al., 1991; Sowell et al., 2004). These changes occur in the context of global increases in white matter volume and decreases in gray matter volume during normal brain development in children (Giedd et al., 1999). Cortical thinning of the PFC during brain maturation may, therefore, be the consequence of synaptic pruning or an increased myelin coating of fibers in the lower cortical layers, or both (Sowell et al., 2004). These anatomical changes in the PFC during adolescence parallel clear cog-

nitive gains in executive functioning, which is thought to depend primarily on the PFC.

The association of higher FSIQ with cortical thinning in regions of the PFC, demonstrated in this study, differs from prior studies, which have largely reported positive correlations of cortical thickness with FSIQ (Karama et al., 2009; Narr et al., 2007; Shaw et al., 2006). In general, however, these studies have not controlled for total brain volume in their methods for measuring cortical thickness or its associations with FSIQ (Karama et al., 2009; Shaw et al., 2006). Given the association of whole brain volume with FSIQ, this would be expected to favor the detection of positive correlations of cortical thickness and FSIQ (McDaniel, 2005; Narr et al., 2007). Previous study has demonstrated inverse correlations of cortical and subcortical volumes with measures of performance on specific cognitive tasks (that correlate strongly with intellectual ability) (Haier et al., 2005a).

The inverse correlations of FSIQ and cortical thickness that we detected suggest that more synaptic pruning or greater myelination may underlie inter-individual differences in intellectual ability. Findings from our analyses of white matter volume, however, help to refine this interpretation. Age exhibited a significant modifying effect on correlations of FSIQ with white matter volumes in the frontal lobe. No significant correlation was detected in children, but FSIQ correlated inversely with right frontal white matter volumes in adults, and this inverse correlation increased in magnitude with increasing age. These correlations indicate that smaller volumes of frontal white matter accompany higher FSIQ scores in adults. Our findings from gray and white matter, therefore, lead us to speculate that synaptic pruning in adults may be more likely to account for inter-individual differences in intellectual ability than the extension of white matter into the cortical neuropil. One would expect that the latter mechanism would feature cortical thinning accompanied by increased volume of underlying white matter. Our findings, however, indicated that intelligence correlated inversely with white matter volumes, suggesting that synaptic pruning in adults more likely accounts for inter-individual differences in intellectual ability. Although the cross-sectional nature of this study limits our ability to infer trajectories of change, our findings would be consistent with different trajectories of brain maturation in adults with average FSIQ versus adults with high or superior FSIQ. Differences in the trajectory of cortical maturation for children and adolescents with average, high, or superior intelligence have previously been demonstrated in a longitudinal imaging study (Shaw et al., 2006); however, no longitudinal study has yet assessed these trajectories in adults.

Although we did not acquire diffusion tensor imaging data in our sample, we attempted to identify the fiber tracts running through the right frontal region of significant interaction by referencing prior fiber tracing studies in human and nonhuman primates (Mori et al., 2005; Schmahmann and Pandya, 2006). The fiber tracts are likely to include the superior longitudinal fasciculus, which connects dorsal frontal with inferior and superior parietal cortices, and the superior corona radiata, which projects reciprocally from the cortex to the thalamus and pontine nuclei. These fiber tracts participate in neural networks that govern a mul-

titude of cognitive functions related to intellectual ability, including attentional and self-regulatory processes (Posner and Rothbart, 2009). The role of white matter fiber tracts, particularly long association fibers, in intellectual performance is supported by findings from lesion studies (Frisoni et al., 2007; Glascher et al., 2010; Turken et al., 2008), proton MRS studies (Jung et al., 2009), and DTI tractography studies (Turken et al., 2008; Yu et al., 2008). White matter integrity, as well as the organizational efficiency of white matter, seems to be important for higher intelligence (Yu et al., 2008).

Several prior imaging studies have demonstrated that males and females differ with respect to the brain features that correlate with intellectual ability. Cortical thickness in prefrontal regions correlates more strongly with intellectual ability in females, whereas males show a stronger correlation in temporal-occipital association cortices (Narr et al., 2007). In our study, correlations of FSIQ with cortical thickness differed for males and females in primarily frontal regions (Broca's area, left cingulate cortex, and right DMPFC), and, in general, females showed a positive correlation, whereas males showed an inverse correlation. Of particular interest is the correlation of FSIQ with cortical thickness in Broca's area in females, which could reflect the female advantage for verbal fluency and a greater contribution of this skill to FSIQ in females than males (Sommer et al., 2004). Broca's area has previously been identified as a region of sex difference in the neuroanatomical correlate of intellectual ability, with females showing correlations of white matter and gray matter volume with intellectual ability in Broca's area (Haier et al., 2005b). Although not examined in this study, other sex differences from prior imaging studies suggest that white matter integrity may be more important for intelligence in females than in males, particularly in later childhood and adulthood (Gur et al., 1999; Haier et al., 2005a; Schmithorst, 2009). Males and females are known to have marked differences in brain size and structure (Luders et al., 2006; Im et al., 2006; Sowell et al., 2007), but similar levels of intellectual ability. Thus, males and females appear to achieve similar levels of intellectual ability through different patterns of brain structure and function.

Our findings contribute to a growing literature concerned with the neurobiological bases of inter-individual differences in intellectual ability. A common pitfall for studies of intellectual ability has been the failure to clearly define intellectual ability and its measures. Confusion frequently surrounds use of the term "general intelligence", which has been used both as a synonym for the *g* factor and as a synonym for a related but distinct concept, "intelligence in general" (Jensen, 1993). The *g* factor (or Spearman's *g*) is derived through identification of the first component from a factor analysis of a given individual's performance on many cognitive tests. As such, it is considered to be "a distillate of the common source of individual differences in all mental tests, completely stripped of their distinctive features of information, content, skill, strategy, and the like" (Jensen, 1998). The *g* factor is a unitary theoretical construct for which no single corresponding biological property or process has yet been identified; however, new research findings suggest that *g* may localize to

a distributed set of regions in the left frontal and right parietal cortex as well as white matter association tracts connecting these sectors (Colom et al., 2006; Deary et al., 2010; Duncan et al., 2000; Glascher et al., 2010; Lee et al., 2006).

Intelligence quotient, in contrast, is a composite measure with high g-loading that derives from performance on a variety of cognitive tasks, including working memory, verbal comprehension, and visuospatial processing. It therefore provides a measure of what has been appropriately termed "intelligence in general" (Jung and Haier, 2007). Functional neuroimaging, neurophysiologic, and lesion studies have shown these various cognitive functions to localize to different brain regions, with working memory based primarily in prefrontal and parietal areas, verbal comprehension in left perisylvian regions, including Broca's and Wernicke's areas, and visuospatial processing in the right parietal lobe (Freedman and Assad, 2009; Glascher et al., 2009; Owen et al., 2005; Vigneau et al., 2006). A comprehensive review of 37 anatomical and functional neuroimaging studies of intelligence has proposed a neurobiological substrate for "intelligence in general" that is based primarily in the frontal and parietal lobes (Jung and Haier, 2007). Thus, the findings of neuroimaging studies of "intelligence in general," including the present study, overlap with the findings from neuroimaging studies of the g-factor, suggesting that frontal and parietal regions compose the primary neurological substrate for g as well as the mental skills specific to a variety of different cognitive tasks.

5. Conclusions, limitations, and future directions

Although this study makes new and distinct contributions to our understanding of the neural basis of intelligence, several methodological and conceptual issues must be considered when interpreting its findings. First, we assessed correlations of cortical thickness with intellectual ability in individuals across a wide age range, from early childhood through mature adulthood. Although this enabled the detection of brain morphological features that were associated with higher FSIQ across childhood and adulthood, it also likely masked important developmental changes in the neural correlates of intelligence. The aggregated sample provided sufficient power to detect several significant correlations and interactions using a highly conservative correction for multiple comparisons; however, once the sample was stratified into smaller groups by sex or age (children under 18 years of age and adults 18 years and older) these findings did not persist, suggesting that the sample was not sufficiently large or optimally distributed by age to detect significant correlations within each age strata. Given the marked changes in brain structure over the life span, as well as sex differences in these patterns of development, our findings will require confirmation by future studies with large samples of children and adults that can be studied in aggregate and also stratified by age and sex. Second, the absence of DTI data in our sample required us to rely on other means for identifying the white matter fiber tracts likely involved in our correlations of white matter volumes with FSIQ. Given the size and

location of the region of significant interaction in the right frontal white matter, however, we regard the referencing of white matter atlases derived from imaging and post-mortem studies as adequate. We were not, however, able to determine the cytoarchitectural determinants for the reduced white matter volumes that were associated with higher FSIQs in adults. In the future, multimodal imaging techniques, incorporating volumetric measures, MRS, DTI, and functional imaging will help to better characterize the role of specific white matter fiber tracts in intellectual functioning. Third, although FSIQ is widely used as a proxy for intellectual ability, it is not a unitary construct, but rather a composite measure that derives from performance on a variety of cognitive tasks. In the future, imaging studies that examine the neural correlates of these specific cognitive abilities, as well as FSIQ, may provide a fuller picture of the neural bases of intellectual ability.

For centuries, scientists have pursued the anatomical and physiological basis for intellectual ability. Brain imaging studies of intellectual ability have generally employed large-scale measures, such as total brain volume or regional gray or white matter volumes (by lobe). Using these metrics, "bigger" appears to be better. Yet, these large-scale measures likely mask subtle differences that may be detected using more refined measures within localized brain regions. Any study of intelligence and localized morphological features of the brain, however, must account for the effects of total brain volume, which has not consistently been the case in studies of cortical thickness and intelligence. We have provided evidence that cortical thinning in portions of the prefrontal cortex may support higher intellectual abilities. Our findings also suggest sex-specific and age-specific patterns in the neuroanatomical features and cellular processes that underlie higher intelligence. Future progress in identifying the multiple neural bases of human intellectual ability will benefit from the integration of anatomical and functional measures of the cortex, white matter, and subcortical nuclei.

References

Arndt, S., Cohen, G., Alliger, R.J., Swayze II, V.W., Andreasen, N.C., 1991. Problems with ratio and proportion measures of imaged cerebral structures. Psychiatry Res. 40, 79–89.

Bansal, R., Staib, L.H., Whiteman, R., Wang, Y.M., Peterson, B.S., 2005. ROC-based assessments of 3D cortical surface-matching algorithms. Neuroimage 24, 150–162.

Bansal, R., Staib, L.H., Xu, D., Zhu, H., Peterson, B.S., 2007. Statistical analyses of brain surfaces using Gaussian random fields on 2-D manifolds. IEEE Trans. Med. Imaging 26, 46–57.

Benes, F.M., Turtle, M., Khan, Y., Farol, P., 1994. Myelination of a key relay zone in the hippocampal formation occurs in the human brain during childhood, adolescence, and adulthood. Arch. Gen. Psychiatry 51, 477–484.

Canivez, G.L., Neitze, l, R., Martin, B.E., 2005. Construct validity of the Kaufman Brief Intelligence Test, Wechsler Intelligence Scale for Children-Third Edition, and Adjustment Scales for Children and Adolescents. J. Psychoed. Assess. 23, 15–34.

Choi, Y.Y., Shamosh, N.A., Cho, S.H., DeYoung, C.G., Lee, M.J., Lee, J.M., Kim, S.I., Cho, Z.H., Kim, K., Gray, J.R., Lee, K.H., 2008. Multiple bases of human intelligence revealed by cortical thickness and neural activation. J. Neurosci. 28, 10323–10329.

Colom, R., Jung, R.E., Haier, R.J., 2006. Finding the g-factor in brain structure using the method of correlated vectors. Intelligence 34, 561–570.

Davatzikos, C., Genc, A., Xu, D., Resnick, S.M., 2001. Voxel-based morphometry using the RAVENS maps: methods and validation using simulation of longitudinal atrophy. Neuroimage 14, 1361–1369.

Deary, I.J., Penke, L., Johnson, W., 2010. The neuroscience of human intelligence differences. Nat. Rev. Neurosci. 11, 201–211.

Duncan, J., Seitz, R.J., Kolodny, J., Bor, D., Herzog, H., Ahmed, A., Newell, F.N., Emslie, H., 2000. A neural basis for general intelligence. Science 289, 457–460.

Freedman, D.J., Assad, J.A., 2009. Distinct encoding of spatial and nonspatial visual information in parietal cortex. J. Neurosci. 29, 5671–5680.

Frisoni, G.B., Galluzzi, S., Pantoni, L., Filippi, M., 2007. The effect of white matter lesions on cognition in the elderly: small but detectable. Nat. Clin. Pract. Neurol. 3, 620–627.

Giedd, J.N., Blumenthal, J., Jeffries, N.O., Castellanos, F.X., Liu, H., Zijdenbos, A., Paus, T., Evans, A.C., Rapoport, J.L., 1999. Brain development during childhood and adolescence: a longitudinal MRI study. Nat. Neurosci. 2, 861–863.

Glascher, J., Tranel, D., Paul, L.K., Rudrauf, D., Rorden, C., Hornaday, A., Grabowski, T., Damasio, H., Adolphs, R., 2009. Lesion mapping of cognitive abilities linked to intelligence. Neuron 61, 681–691.

Gogtay, N., Giedd, J.N., Lusk, L., Hayashi, K.M., Greenstein, D., Vaituzis, A.C., Nugent III, T.F., Herman, D.H., Clasen, L.S., Toga, A.W., Rapoport, J.L., Thompson, P.M., 2004. Dynamic mapping of human cortical development during childhood through early adulthood. Proc. Natl. Acad. Sci. U.S.A. 101, 8174–8179.

Gould, S.J., 1981. The Mismeasure of Man. W.W. Norton & Company, Inc., New York.

Gur, R.C., Turetsky, B.I., Matsui, M., Yan, M., Bilker, W., Hughett, P., Gur, R.E., 1999. Sex differences in brain gray and white matter in healthy young adults: correlations with cognitive performance. J. Neurosci. 19, 4065–4072.

Haier, R.J., Jung, R.E., Yeo, R.A., Head, K., Alkire, M.T., 2005a. The neuroanatomy of general intelligence: sex matters. Neuroimage 25, 320–327.

Haier, R.J., Jung, R.E., Yeo, R.A., Head, K., Alkire, M.T., 2005b. Structural brain variation, age, and response time. Cogn. Affec. Behav. Neurosci. 5, 246–251.

Huttenlocher, P.R., 1990. Morphometric study of human cerebral cortex development. Neuropsychologia 28, 517–527.

Huttenlocher, P.R., Dabholkar, A.S., 1997. Regional differences in synaptogenesis in human cerebral cortex. J. Comp. Neurol. 387, 167–178.

Im, K., Lee, J.M., Lee, J., Shin, Y.W., Kim, I.Y., Kwon, J.S., Kim, S.I., 2006. Gender difference analysis of cortical thickness in healthy young adults with surface-based methods. Neuroimage 31, 31–38.

Jensen, A.R., 1993. Spearman's g: links between psychometrics and biology. Ann. NY Acad. Sci. 702, 103–129.

Jensen, A.R., 1998. The g Factor: The Science of Mental Abilities. Praeger, Westport, CT.

Jernigan, T.L., Trauner, D.A., Hesselink, J.R., Tallal, P.A., 1991. Maturation of human cerebrum observed in vivo during adolescence. Brain 114, 2037–2049.

Jung, R.E., Haier, R.J., 2007. The Parieto-Frontal Integration Theory (P-FIT) of intelligence: converging neuroimaging evidence. Behav. Brain Sci. 30, 135–154.

Jung, R.E., Gasparovic, C., Chavez, R.S., Caprihan, A., Barrow, R., Yeo, R.A., 2009. Imaging intelligence with proto magnetic resonance spectroscopy. Intelligence 37, 192–198.

Karama, S., Ad-Dab'bagh, Y., Haier, R.J., Deary, I.J., Lyttelton, O.C., Lepage, C., Evans, A.C., the Brain Development Cooperative Group, 2009. Positive association between cognitive ability and cortical thickness in a representative US sample of healthy 6 to 18 year-olds. Intelligence 37, 145–155.

Kaufman, A., Kaufman, J., Balgopaland, R., McLean, J., 1996. Comparison of three WISC-III short forms: weighing psychometric, clinical, and practical factors. J. Clin. Child. Psychol. 25, 97–105.

Kaufman, J., Birmaher, B., Brent, D., Rao, U., Flynn, C., Moreci, P., Williamson, D., Ryan, N., 1997. Schedule for Affective Disorders and Schizophrenia for School-Age Children—Present and Lifetime Version (K-SADS-PL): initial reliability and validity data. J. Am. Acad. Child. Adolesc. Psychiatry 36, 980–988.

Lee, K.H., Choi, Y.Y., Gray, J.R., Cho, S.H., Chae, J.H., Lee, S., Kim, K., 2006. Neural correlates of superior intelligence: stronger recruitment of posterior parietal cortex. Neuroimage 29, 578–586.

Luders, E., Narr, K.L., Thompson, P.M., Rex, D.E., Woods, R.P., Deluca, H., Jancke, L., Toga, A.W., 2006. Gender effects on cortical thickness and the influence of scaling. Hum. Brain Mapp. 27, 314–324.

Luders, E., Narr, K.L., Thompson, P.M., Toga, A.W., 2009. Neuroanatomical correlates of intelligence. Intelligence 37, 156–163.

McDaniel, M.A., 2005. Big-brained people are smarter: a meta-analysis of the relationship between in vivo brain volume and intelligence. Intelligence 33, 337–346.

Mori, S., Wakana, S., Nagae-Poetscher, L.M., van Zijl, P.C.M., 2005. MRI Atlas of Human White Matter. Elsevier, Amsterdam.

Narr, K.L., Woods, R.P., Thompson, P.M., Szeszko, P., Robinson, D., Dimtcheva, T., Gurbani, M., Toga, A.W., Bilder, R.M., 2007. Relationships between IQ and regional cortical gray matter thickness in healthy adults. Cereb. Cortex 17, 2163–2171.

Neisser, U., Boodoo, G., Bouchard, T.J., Boykin, A.W., Brody, N., Ceci, S.J., Halpern, D.F., Loehlin, J.C., Perloff, R., Sternberg, R.J., Urbina, S., 1996. Intelligence: knowns and unknowns. Am. Psychol. 51, 77–101.

Owen, A.M., McMillan, K.M., Laird, A.R., Bullmore, E., 2005. N-back working memory paradigm: a meta-analysis of normative functional neuroimaging studies. Hum. Brain Mapp. 25, 46–59.

Peterson, B.S., 2010. Form determines function: new methods for identifying the neuroanatomical loci of circuit-based disturbances in childhood disorders. J. Am. Acad. Child Adolesc. Psychiatry 49, 533–538.

Posner, M.I., Rothbart, M.K., 2009. Toward a physical basis of attention and self-regulation. Phys. Life Rev. 6, 103–120.

Psychological Corporation, 1999. Wechsler Abbreviated Scale of Intelligence (WASI), Technical Manual. Psychological Corporation, San Antonio, TX.

Schmahmann, J.D., Pandya, D.N., 2006. Fiber Pathways of the Brain. Oxford University Press, New York.

Schmithorst, V.J., 2009. Developmental sex differences in the relation of neuroanatomical connectivity to intelligence. Intelligence 37, 164–173.

Shattuck, D.W., Leahy, R.M., 2002. BrainSuite: an automated cortical surface identification tool. Med. Image. Anal. 6, 129–142.

Shaw, P., Greenstein, D., Lerch, J., Clasen, L., Lenroot, R., Gogtay, N., Evans, A., Rapoport, J., Giedd, J., 2006. Intellectual ability and cortical development in children and adolescents. Nature 440, 676–679.

Sled, J.G., Zijdenbos, A.P., Evans, A.C., 1998. A nonparametric method for automatic correction of intensity nonuniformity in MRI data. IEEE Trans. Med. Imaging 17, 87–97.

Sommer, I.E., Aleman, A., Bouma, A., Kahn, R.S., 2004. Do women really have more bilateral language representation than men? A meta-analysis of functional imaging studies. Brain 127, 1845–1852.

Sowell, E.R., Thompson, P.M., Holmes, C.J., Batth, R., Jernigan, T.L., Toga, A.W., 1999a. Localizing age-related changes in brain structure between childhood and adolescence using statistical parametric mapping. Neuroimage 9, 587–597.

Sowell, E.R., Thompson, P.M., Holmes, C.J., Jernigan, T.L., Toga, A.W., 1999b. In vivo evidence for post-adolescent brain maturation in frontal and striatal regions. Nat. Neurosci. 2, 859–861.

Sowell, E.R., Thompson, P.M., Leonard, C.M., Welcome, S.E., Kan, E., Toga, A.W., 2004. Longitudinal mapping of cortical thickness and brain growth in normal children. J. Neurosci. 24, 8223–8231.

Sowell, E.R., Peterson, B.S., Kan, E., Woods, R.P., Yoshii, J., Bansal, R., Xu, D., Zhu, H., Thompson, P.M., Toga, A.W., 2007. Sex differences in cortical thickness mapped in 176 healthy individuals between 7 and 87 years of age. Cereb. Cortex 17, 1550–1560.

Spitzer, R.L., Williams, J.B.W., Gibbon, M., First, M.B., 1992. The Structured Clinical Interview for DSM-III-R (SCID). Arch. Gen. Psychiatry 49, 624–629.

Turken, A., Whitfield-Gabrieli, S., Bammer, R., Baldo, J.V., Dronkers, N.F., Gabrieli, J.D., 2008. Cognitive processing speed and the structure of white matter pathways: convergent evidence from normal variation and lesion studies. Neuroimage 42, 1032–1044.

Vigneau, M., Beaucousin, V., Herve, P.Y., Duffau, H., Crivello, F., Houde, O., Mazoyer, B., Tzourio-Mazoyer, N., 2006. Meta-analyzing left hemisphere language areas: phonology, semantics, and sentence processing. Neuroimage 30, 1414–1432.

Wells III, W.M., Viola, P., Atsumi, H., Nakajima, S., Kikinis, R., 1996. Multimodal volume registration by maximization of mutual information. Med. Image Anal. 1, 35–51.

Wood, J.N., Grafman, J., 2003. Human prefrontal cortex: processing and representational perspectives. Nat. Rev. Neurosci. 4, 139–147.

Xu, D., Hao, X., Bansal, R., Plessen, K.J., Geng, W., Hugdahl, K., Peterson, B.S., 2007. Unifying the analyses of anatomical and diffusion tensor images using volume-preserved warping. J. Magn. Reson. Imaging 25, 612–624.

Yu, C., Li, J., Liu, Y., Qin, W., Li, Y., Shu, N., Jiang, T., Li, K., 2008. White matter tract integrity and intelligence in patients with mental retardation and healthy adults. Neuroimage 40, 1533–1541.